

# Anomalous synchronization threshold in coupled logistic maps

C. Anteneodo

*Departamento de Física, Pontifícia Universidade Católica do Rio de Janeiro,  
Caixa Postal 38071, 22452-970 RJ, Rio de Janeiro, Brazil*

A. M. Batista

*Departamento de Matemática e Estatística, Universidade Estadual de Ponta Grossa, 84030-900 PR, Ponta Grossa, Brazil*

R. L. Viana

*Departamento de Física, Universidade Federal do Paraná, 81531-990 PR, Curitiba, Brazil*

We consider regular lattices of coupled chaotic maps. Depending on lattice size, there may exist a window in parameter space where complete synchronization is eventually attained after a transient regime. Close outside this window, an intermittent transition to synchronization occurs. While asymptotic transversal Lyapunov exponents allow to determine the synchronization threshold, the distribution of finite-time Lyapunov exponents, in the vicinity of the critical frontier, is expected to provide relevant information on phenomena such as intermittency. In this work we scrutinize the distribution of finite-time exponents when the local dynamics is ruled by the logistic map  $x \mapsto 4x(1-x)$ . We obtain a theoretical estimate for the distribution of finite-time exponents, that is markedly non-Gaussian. The existence of correlations, that spoil the central limit approximation, is shown to modify the typical intermittent bursting behavior. The present scenario could apply to a wider class of systems with different local dynamics and coupling schemes.

PACS numbers: 05.45.Ra, 05.45.-a, 05.45.Xt

## I. INTRODUCTION

Coupled map lattices (CMLs), dynamical systems with discrete space and time, are being intensively investigated since the early 80's as models of many spatiotemporal phenomena occurring in a wide variety of systems [1]. One of such phenomena is synchronization and, in particular, amongst the various kinds of synchronized behavior, *complete synchronization* (CS) [2] occurring in regular arrays of coupled chaotic systems. Intermittency plays an important role in the destabilization of the synchronized state[3]. Intermittent transitions between laminar, quiescent states, and irregular bursting have been investigated in many dynamical systems, their scaling properties being determined[4, 5, 6]. Theoretical derivations of these scalings usually assume Gaussian fluctuations for describing the irregular bursts between consecutive laminar regions. Although this may be a suitable approximation for many systems, there are cases where deviations from Gaussianity can be observed, specially in the vicinity of the synchronization threshold. It is our purpose to exhibit such anomalous behavior.

Let us consider, as paradigmatic example of a spatially extended system, periodic chains of  $N$  one-dimensional chaotic maps  $x \mapsto f(x)$  evolving through a distance-dependent diffusive coupling:

$$x_{t+1}^{(i)} = (1-\varepsilon)f(x_t^{(i)}) + \frac{\varepsilon}{\eta} \sum_{r=1}^{N'} B(r) \left( f(x_t^{(i-r)}) + f(x_t^{(i+r)}) \right), \quad (1)$$

where  $x_t^{(i)}$  represents the state variable for the site  $i$  ( $i = 1, 2, \dots, N$ ) at time  $t$ ,  $\varepsilon \geq 0$  is the coupling strength,

$B(r)$  an arbitrary function of  $r$  and  $\eta = 2 \sum_{r=1}^{N'} B(r)$  a normalization factor, with  $N' = (N-1)/2$  for odd  $N$ .

CS takes place when the dynamical variables that define the state of each map adopt the same value for all the coupled maps at each time step  $t$ , i.e.,  $x_t^{(1)} = x_t^{(2)} = \dots = x_t^{(N)} \equiv x_t^{(*)}$ . It can be easily verified that this state is solution of Eq. (1). The question is whether it is stable or not with respect to small perturbations in directions transversal to the CS state in CML phase space. A criterion for stability can be drawn from the asymptotic Lyapunov spectrum (LS). As far as the CS state lies along the direction associated to the largest exponent, the CS state will be transversely stable if the  $(N-1)$  remaining exponents are negative. Therefore, if there is a single attractor, negativity of the second largest Lyapunov exponent implies that the CS state is asymptotically attained[7]. Depending thus on system size and on the parameters defining both the chaotic map and  $B(r)$ , there may exist an interval of values of the coupling strength  $\varepsilon$  for which the CS state is asymptotically stable. Explicit results have been shown before, for instance, for algebraically decaying interactions, i.e.,  $B(r) = 1/r^\alpha$ , with  $0 \leq \alpha[8, 9]$  and for uniform interactions with a cut-off distance  $\beta$ , with  $1 \leq \beta \leq N'[10]$ . In those cases, for a given system size, one finds a *synchronization domain* in parameter space.

Inside this domain, CS eventually occurs after a transient whose typical duration diverges as one approaches the critical frontier. Outside the synchronization domain, there may occur intermittent behavior. A characterization of phenomena associated to a blowout bifurcation, such as intermittency[11], can be performed through the

analysis of the distribution of largest transversal finite-time Lyapunov exponents (LTFEs). We will show that for Ulam maps coupled through schemes of the form (1), the probability density function (PDF) of LTFEs deviates from a Gaussian law. This will be shown to have important consequences at criticality. Let us remark that analytical results are specially relevant in this field due to the very nature of the phenomena involved, sensitive to the unavoidable finite precision of numerical simulations [12].

## II. FINITE-TIME LYAPUNOV SPECTRUM

The dynamics of tangent vectors  $\xi = (\delta x^{(1)}, \delta x^{(2)}, \dots, \delta x^{(N)})^T$  is obtained by differentiation of the evolution equations (1). In order to obtain finite-time exponents, we proceed analogously to what we have done before for the calculation of asymptotic exponents [8, 9]. For self-containedness, let us review the steps. The tangent dynamics is given by  $\xi_{i+1} = \mathbf{T}_i \xi_i$ , where the Jacobian matrix  $\mathbf{T}_i$  is

$$\mathbf{T}_i = \left( (1 - \varepsilon) + \frac{\varepsilon}{\eta} \mathbf{B} \right) \mathbf{D}_i, \quad (2)$$

with the matrices  $\mathbf{D}_i$  and  $\mathbf{B}$  defined, respectively, by  $D_i^{jk} = f'(x_i^{(j)})\delta_{jk}$  and  $B_{jk} = B(r_{jk})(1 - \delta_{jk})$ , being  $r_{jk} = \min_{l \in \mathcal{Z}} |j - k + lN|$ . Once the initial conditions have been specified, the LS of finite-time Lyapunov exponents (FTEs)  $\{\bar{\lambda}_k(n)\}$ , calculated over a time interval of length  $n$ , is extracted from the evolution of the initial tangent vector  $\xi_0$ :  $\xi_n = \mathcal{T}_n \xi_0$ , where  $\mathcal{T}_n \equiv \mathbf{T}_{n-1} \dots \mathbf{T}_1 \mathbf{T}_0$ . The FTEs are obtained as  $\bar{\lambda}_k(n) = \ln \bar{\Lambda}_n^{(k)}$ , for  $k = 1, \dots, N$ , where  $\{\bar{\Lambda}_n^{(k)}\}$  are the eigenvalues of  $\hat{\Lambda}_n = (\mathcal{T}_n^T \mathcal{T}_n)^{\frac{1}{2n}}$  [13].

In CS states, the dynamical variables of all maps coincide at each time step  $i$ , i.e.,  $x_i^{(1)} = x_i^{(2)} = \dots = x_i^{(N)} \equiv x_i^{(*)}$ . In this case,  $\mathbf{D}_i = f'(x_i^{(*)}) \mathbf{1}_N$ , thus,  $\mathbf{T}_i = f'(x_i^{(*)}) \mathbf{B}$  and  $\mathcal{T}_i^T \mathcal{T}_i = (\prod_{j=0}^{i-1} [f'(x_j^{(*)})]^2) \mathbf{B}^{2i}$ . Therefore, one arrives at the following expression for the spectrum of  $N$  finite-time Lyapunov exponents, over a time interval of length  $n$ , in CS states:

$$\lambda_k(n) = \frac{1}{n} \sum_{i=0}^{n-1} \ln |f'(x_i^{(*)})| + c_k, \quad \text{for } k = 1, \dots, N, \quad (3)$$

with  $c_k \equiv \ln |1 - \varepsilon + \varepsilon b_k / \eta|$ , where  $b_k$ , the eigenvalues of the interaction matrix  $\mathbf{B}$ , are given by  $b_k = 2 \sum_{m=1}^{N'} B(m) \cos(2\pi k m / N)$ , for odd  $N$ . Here  $x_i^{(*)} = f^i(x_0^{(*)})$  is the  $i$ th iterate of the initial condition  $x_0^{(*)}$ , the same for the  $N$  maps, since we are dealing with CS states.

In the asymptotic case  $n \rightarrow \infty$ , and assuming ergodicity, the first term in the left-hand side of Eq. (3), which represents a time-average, can be substituted by an average over the single-map attractor. In such case one gets the asymptotic LS

$$\lambda_k = \lambda_U + c_k, \quad (4)$$

where  $\lambda_U = \langle \ln |f'(x^{(*)})| \rangle$  is the Lyapunov exponent of the uncoupled map. Notice that the parameters that define the particular uncoupled map affect only  $\lambda_U$ , while  $\{c_k\}$  are determined by the particular cyclic dependence on distance in the regular coupling scheme.

As discussed in the Introduction, the asymptotic LS provides a criterion for synchronization, namely the negativity of second largest (or largest transversal) asymptotic exponent  $\lambda_{\perp}$ . For the particular interaction  $B(r) = 1/r^\alpha$ , that we will consider in numerical simulations, the above condition leads to [8, 9]

$$\frac{1 - e^{-\lambda_U}}{1 - b_1/\eta} < \varepsilon < \frac{1 + e^{-\lambda_U}}{1 - b_{N'}/\eta}. \quad (5)$$

## III. DISTRIBUTION OF FINITE-TIME LYAPUNOV EXPONENTS

Unlike infinite-time exponents, local exponents strongly depend on the initial conditions. Starting from random initial conditions, the fluctuations in the values of  $\lambda_k(n)$  arise from the summation in (3) only, since  $\{c_k\}$  are constant. As a consequence, all the  $\lambda_k(n)$  of the spectrum will have a PDF with the same shape, differing only in the mean value  $\langle \lambda_k(n) \rangle = \lambda_U + c_k$ , which coincides with the asymptotic exponent  $\lambda_k$ . In particular the variance of finite-time Lyapunov exponents (FTEs) in the CS states does not depend on  $c_k$  (since it is an additive constant). Therefore, it is the same for all the exponents of the spectrum, as expected also from the fact that the source of the fluctuations is unique. Along a trajectory, fluctuations shift the finite-time Lyapunov spectrum as a whole. A further consequence is that the variance of the local exponents in CS states does not depend on the lattice parameters embodied in  $\{c_k\}$ , but only on the local features of the individual map. In fact, in CS states, all maps evolve with the dynamics of an uncoupled map. Being so, the PDFs of FTEs can be straightforwardly obtained from the PDF of the local map. Hence, let us omit by the moment the index  $k$ . Our discussion will be valid for any  $\lambda_k(n)$ , in particular for  $\lambda_{\perp}(n)$ .

For the Ulam map,  $x \mapsto 4x(1 - x)$ , a smooth approximate expression for the PDF of FTEs is available [14], namely

$$P(\lambda(n)) \simeq \frac{2n}{\pi^2} \ln(\coth |n[\lambda(n) - \lambda]/2|), \quad (6)$$

valid for large enough  $n$ . For  $\lambda(n) < \lambda$ , expression (6) is exact, however, for  $\lambda(n) > \lambda$ , the exact distribution presents a complex structure with  $2^{n-1}$  spikes that get narrower and accumulate close to the mean value with increasing  $n$  [14, 15]. Therefore, in the latter interval, expression (6) constitutes a smooth approximation, such that the sharp spikes have been trimmed by finite size bins. Moreover, the exact PDF is non-null only for  $\lambda(n) - \lambda \leq \ln 2$ .

Even the smooth distribution (6) is markedly different from Gaussian. It is divergent at  $\lambda(n) = \lambda$  and falls off with exponential tails. It is noteworthy that the variance decays anomalously as  $1/n^2$  [14, 16]

$$\sigma^2(n) = \frac{\pi^2}{6n^2} \left(1 - \frac{1}{2^n}\right), \quad (7)$$

instead of the usual  $1/n$  decay. Also notice that the PDFs (6) for different values of  $n$  would collapse into a single shape via rescaling by  $n$ .

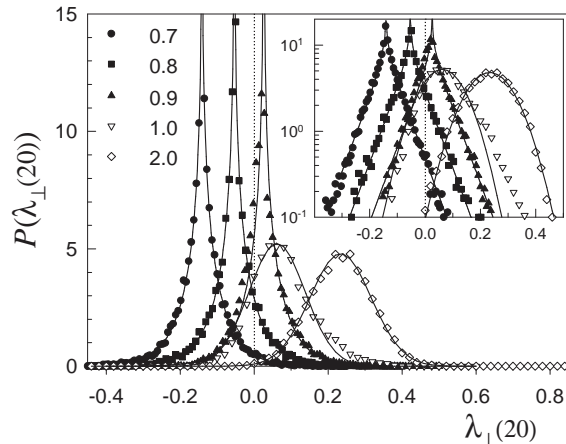


FIG. 1: Comparison between numerical and theoretical PDFs. They correspond to the largest transversal time-20 exponent of  $N = 21$  coupled Ulam maps, with algebraically decaying interactions, for  $\varepsilon = 0.8$  and different values of  $\alpha$  (above  $\alpha_c \simeq 0.867$  stability of the CS state is lost). Numerical PDFs are represented by symbols. Solid lines associated to full symbols correspond to the theoretical prediction given by Eq. (6), while those associated to hollow symbols correspond to Gaussian fittings. Inset: semi-log representation to exhibit the tails.

Fig. 1 exhibits numerical PDFs for CMLs together with the analytical prediction given by Eq. (6). Numerical PDFs were built by choosing  $10^4$  initial conditions and computing the second eigenvalue of the matrix  $\hat{\Lambda}_n$  after a transient. Eq. (6), obtained for uncoupled maps, is in excellent agreement with numerical results for LTFEs in the coherent states of CMLs, as expected. It is worth noting that, although expression (6) was derived for CS states, it remains still a good approximation even close outside the synchronization domain. This means that the correlations that lead to violation of the central limit theorem persist in that region. However, far enough from the threshold, the terms that contribute to FTEs become uncorrelated by the “bath” of coupled chaotic maps, and the central limit theorem holds, leading to Gaussian shapes (see Fig. 1). Notice that the PDF for  $\alpha = 1.0$ , although Gaussian in the central part, stills falls at right with a exponential tail. A detailed analysis of correlations giving rise to (6) can be found in Refs. [14, 16]. Basically,

the autocorrelation function  $C(n)$  of one-step FTEs is  $C(n) = -\pi^2 2^{-n}/24$ , that is, it decays exponentially with time  $n$  (with a characteristic time equal to the inverse of  $\lambda_U = \ln 2$ ). However, since successive one-step exponents are dependent through the deterministic logistic mapping, non-Gaussian PDFs of FTEs arise.

## IV. CONSEQUENCES OF FLUCTUATING EXPONENTS

### A. Subcritical regime

For parameter values belonging to the synchronization domain, that is, for subcritical  $\alpha$ , being all other parameters fixed, the system eventually converges to the CS state. In fact, asymptotically, CS states are stable since the distribution of LTFEs collapses to a Dirac delta function centered at  $\lambda_\perp$ , which is negative in that domain. The relaxation to a CS state can be measured, for instance, by means of either the distance to the SM, defined through  $d(t) = \sqrt{\sum_i (x_t^{(i)} - \langle x_t \rangle)^2}$ , or the order parameter  $R(t) = |\sum_i \exp(2\pi x_t^{(i)})|/N$ . Since, for small deviations from the SM, both quantities are related through  $d^2 \simeq (1 - R^2)/2$ , we will exhibit the time evolution of  $d^2$  only. After a very brief transient, the decay to the CS state is exponential with a characteristic time given by  $\tau_c = 1/|\lambda_\perp|$  (see Fig. 2), that diverges at the critical frontier. For the power-law interaction,  $\lambda_\perp$  scales as  $|\lambda_\perp| \sim |\alpha - \alpha_c|$  and  $|\lambda_\perp| \sim |\varepsilon - \varepsilon_c|$ , at the critical point.

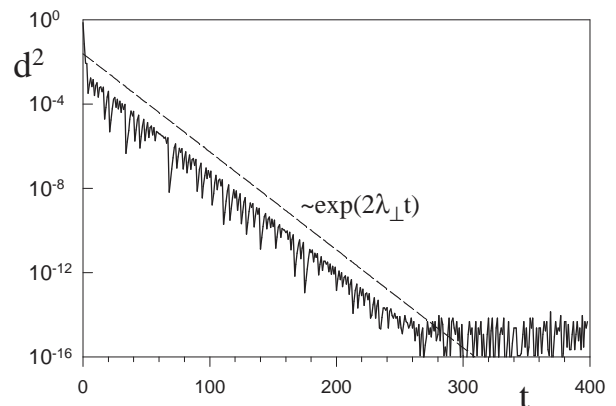


FIG. 2: Relaxation to the synchronization manifold. Time series of  $d^2$  for the same CML of Fig. 1 with  $\alpha = 0.8$  (subcritical). The dashed line corresponds to the exponential law indicated in the figure, for comparison.

The fact that the distribution of LTFEs spreads over negative and positive values (Fig. 1), implies that the exponents, computed over finite-time segments of a trajectory, fluctuate around zero. On one hand, as one approaches the frontier subcritically, the mean value of

the distribution shifts to zero from negative values. On the other hand, as one follows a trajectory for a longer time interval, the PDF of LTFEs concentrates around the mean. Then, there may be segments of trajectory in which the lattice is repelled from the synchronization manifold (SM). But, in average, it is attracted exponentially fast. Due to the finite precision of computer calculations, the distance to the SM saturates (see Fig. 2). Intrinsic noise, due to numerical truncation, may drive the state of the system slightly away from the saturation level. However, each time this happens, the distance decays, again exponentially fast, to its lower bound.

Numerical results in the subcritical regime, illustrated in Fig. 2, can be suitably described by  $d(t) = d_o \exp[\lambda_\perp(t)t]$ . Then, from Eq. (3), we have

$$d(t) = d_o \exp[\lambda_\perp t + \sum_{n=0}^t \zeta(n)] \quad (8)$$

where we have split the fluctuating component  $\zeta = \lambda_\perp(1) - \lambda_\perp$ , corresponding to successive (time-correlated) centered one-step LTFEs. The evolution of the distance to the SM can also be modeled by a Itô multiplicative stochastic differential equation for  $d$ ,

$$\dot{d} = \lambda_\perp d + \zeta(t)d, \quad (9)$$

where  $\zeta(t)$  is a colored non-Gaussian noise and time is continuous.

As shown in Sect. III, in particular, the distribution of  $\lambda_\perp(1)$  in synchronized states follows that of one-step FTEs in the uncoupled map. An exact expression can be straightforwardly derived from the invariant measure of the Ulam attractor[15]. Then, one has

$$P(\zeta) = \frac{2}{\pi} \frac{1}{\sqrt{4e^{-2\zeta} - 1}}, \quad (10)$$

with  $\zeta \in (-\infty, \ln 2)$ . Notice that  $\zeta$ , with zero-mean, is bounded from above. This explains the upper bound of the fluctuations superposed to the exponential decay in Fig. (2). In fact, the fluctuations around the exponential envelope can be fully described by the statistics of time-one exponents. The time series and distribution of  $\zeta$  are presented in Fig. 3 for supercritical  $\alpha$ , showing that even close outside the synchronization domain, the distribution of  $\zeta$  follows that of the uncoupled map.

Breakdown of shadowability might occur[17], as exponents fluctuating about zero are a signature of unstable dimension variability. Taking into account that the PDF is non-null for  $\lambda_\perp(n) \leq \lambda_\perp + \ln 2$ [14, 15], then if  $\lambda_\perp(\alpha, \varepsilon, N) < -\ln 2$ , the finite-time exponents are negative for almost any initial condition. Thus, this point would correspond to the onset of shadowability. Whereas, for  $-\ln 2 < \lambda_\perp$ , although the mean of the distribution may be negative, there is always a non-null fraction  $f$  of positive exponents given by  $f = \int_0^\infty d\lambda_\perp(n) P(\lambda_\perp(n))$ , pointing to the possibility of loss of shadowability of numerical trajectories[18]. Because  $f$

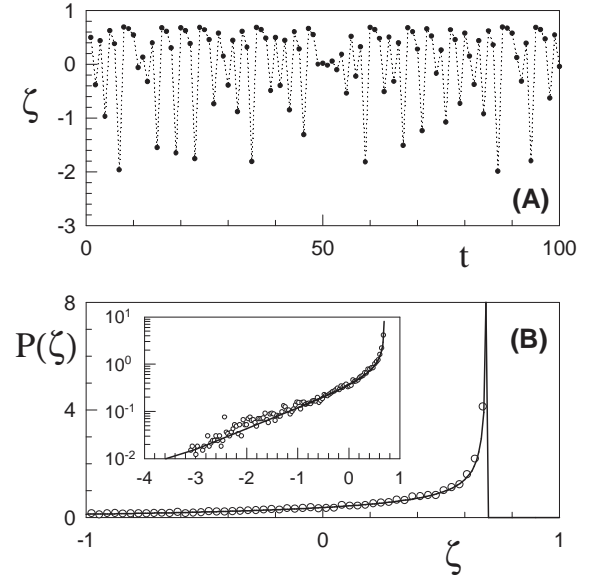


FIG. 3: Time evolution of  $\zeta = \lambda_\perp(1) - \lambda_\perp$  (A) for the same CML of Fig. 1 with  $\alpha = 0.9$  (supercritical). Normalized histogram of  $\zeta$  (B). Inset: semi-log representation to exhibit the exponential tail. Full lines correspond to Eq. (10).

grows from zero with a very small slope, since the positive tail of the PDF is approximately exponential, then the onset may appear shifted towards the threshold in numerical computations[19].

## B. Supercritical regime

For supercritical  $\alpha$ , that is outside the synchronization domain, CS states are not asymptotically stable, because  $\lambda_\perp > 0$ . Close to the threshold (up to  $\alpha \simeq 1$  for  $\epsilon = 0.8$ ), the numerical estimate for the second largest transversal exponent fairly coincides with  $\lambda_\perp$  (calculated for synchronized states). Moreover, close enough to the boundary, correlated bursts away from the SM occur (see Fig. 4). Although this figure exhibits a time series up to  $t = 2000$ , the same features are observed for longer runs (performed typically up to  $t = 10^7$ ).

The intermittent behavior can also be understood in terms of the distribution of the finite-time largest transversal exponent  $\lambda_\perp(n)$ , that close to the threshold can be described by Eq. (6). Although the average  $\langle \lambda_\perp(n) \rangle = \lambda_\perp$  is positive, there is a non-null probability that the LTFE be negative, thus leading to intermittent behavior at finite times. The distribution of LTFEs indicates that there are time intervals during which the trajectories are either attracted to or repelled from the SM. Despite the average duration of the synchronized time in-

tervals increases when approaching the critical frontier, synchronization is not attained as a final stable state.

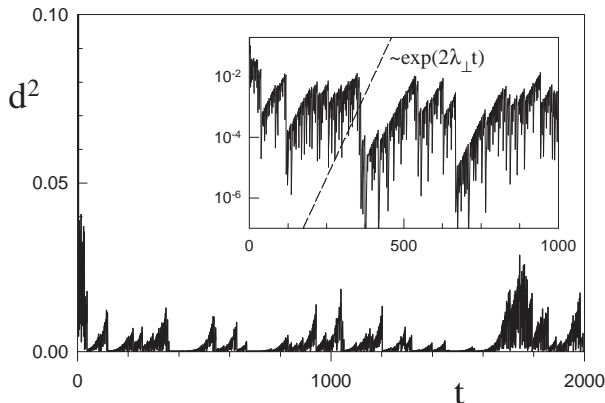


FIG. 4: Time series of  $d^2$  for the same CML of Fig. 1 with  $\alpha \simeq 0.9$  (supercritical). Inset: semi-log representation of the same data. The dashed line corresponds to the exponential law indicated in the figure, for comparison.

Intermittent bursts grow exponentially with a characteristic time given by  $1/\lambda_\perp$  (see inset of Fig. 4). Therefore, the characteristic time has the same scaling laws as the subcritical characteristic time discussed above. The distance to the SM fluctuates around a reference level ( $\langle d \rangle \simeq 0.037$  for the parameters in Fig. 4) that increases with  $\alpha$ . Nonlinearities in Eq. (9) cause saturation of the growth experienced by the distance to the SM due to the positiveness of  $\lambda_\perp$ , and keep the distances within a bounded interval. Close to the threshold, the average distance increases linearly with  $\lambda_\perp \sim |\alpha - \alpha_c|$ . Also, for increasing  $\alpha$ , the correlated bursts become more frequent (hence, its duration becomes shorter) such that far from the frontier fluctuations become uncorrelated and the intermittent clustering effect disappears. Moreover, in that region, the numerical estimate of the largest transversal exponent significantly deviates from the one calculated for synchronized states and new features, out of the scope of the present work, occur. Therefore, we will focus on the near vicinity of the threshold.

The histogram of logarithmic distances  $y \equiv \ln d$  is presented in Fig. 5. The distribution initially grows approximately as  $\exp(ay)$  and above the maximum value falls off faster than exponentially. The coefficient of the exponential argument is  $a \simeq 1$ , at variance, with the value  $a = 2\lambda_\perp/\sigma_1^2 \equiv h$  (hyperbolicity exponent)[6], where  $\sigma^2$  is the variance of time-1 exponents, derived under assumption of Gaussian fluctuations. In fact, in the continuum approximation, the evolution of  $y \equiv \ln d$  follows, at first order, the Langevin equation

$$\dot{y} = \lambda_\perp + \zeta(t) \quad (11)$$

where  $\zeta$  is a fluctuating quantity with zero-mean and variance  $\sigma_1^2$ . If fluctuations were white Gaussian ones, then, from the stationary solution of its associated Fokker-Planck equation, the distribution of  $y$  should increase following the law  $P(y) \sim \exp(hy)$ , with  $h$  defined as above. Multiplicative corrections to Eq. (11), to model the upper-bounded behavior of  $d$ , will affect the shape of  $P(y)$  mainly above the average value, and are not expected to affect the small  $d$  behavior. The main point is that the stochastic process  $\{\zeta\}$  is not white nor Gaussian, as can be neatly observed in Fig. 3, what may explain the deviation from the  $\exp(hy)$  law.

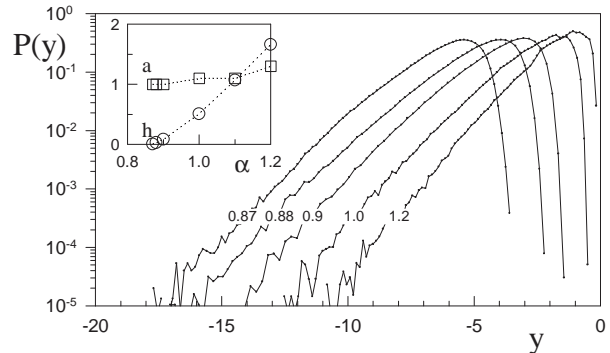


FIG. 5: Distribution of the logarithmic distance  $y = \ln d$ , for different values of  $\alpha$ . Inset: exponent  $a$ , resulting from the best exponential fit to the initial increasing regime, and hyperbolicity exponent  $h$  and as a function of  $\alpha$ .

A universal result is that, at the onset of intermittency, the distribution of laminar phases (inter-burst intervals) decays as a power-law[4], meaning the presence of lengths of arbitrarily large size. In particular the size of the average plateau diverges. Moving far from the onset, the tail of the distribution of laminar phases is gradually dominated by an exponential decay. In general, the distribution of lamellar phases can be obtained by solving a first-return problem. For the power-law decay, the exponent  $\beta = 3/2$  was found to be universal, as far as the central limit approximation holds[4]. However, as we have seen, in our case, very close to the threshold, correlations persist and the distribution of finite-time exponents, even, and specially, in the central part (where it is divergent), deviates from the Gaussian approximation. Therefore, deviations from the  $3/2$  power law are expected. We measured inter-burst sizes, that is, the length of time segments during which the distance  $d$  remains below a threshold value  $d_o$ . Numerical distributions of inter-burst sizes, for values of parameter  $\alpha$  close to the synchronization threshold, are displayed in Fig. 6. In general, a rapid decay is observed for very small  $\tau$  (not exhibited). Since a power-law behavior is expected for sufficiently large  $\tau$ , histogram heights for small values of  $\tau$  are not exhibited in the figure, for the sake of clearness. One sees that the PDF of inter-burst intervals

follows a power-law with  $\beta \simeq 1$ , at neat variance with the value  $\beta = 3/2$ . A cross-over to a asymptotic exponential regime is always observed. We have already seen in Fig. 1 that, below  $\alpha \simeq 1$ , correlations persist. This may explain the power-law exponent observed in Fig. 5.

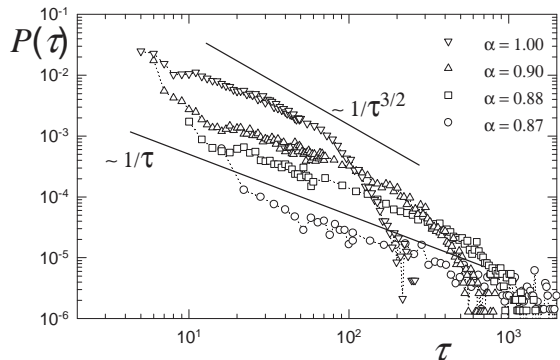


FIG. 6: Distribution of inter-burst times for the same CML of Fig. 1 with different (supercritical) values of  $\alpha$  indicated on the graph. In all cases,  $d_o \simeq 2\langle d \rangle$ , but we verified that decay laws do not substantially depend on the choice of the threshold  $d_o$ . Full lines, corresponding to the indicated power-laws, were drawn for comparison.

## V. SUMMARY

We have presented analytical results for the PDF of LTFEs in CS states of coupled Ulam maps. They were confirmed by numerical experiments performed for CMLs with interactions decaying with distance as a power law. The knowledge of the statistical properties of finite-time Lyapunov exponents allows to understand the anomalies in bursting behavior close to the SM. As a consequence, universal laws derived under assumption of Gaussian fluctuations do not hold generically.

Our results were obtained for local Ulam maps, however, the observed features may occur in a wider class of extended systems, as long as other deterministic chaotic or stochastic processes present similar deviations from Gaussianity[15].

## Acknowledgments

This work was partially supported by Brazilian agencies CNPq and Fundação Araucária.

- 
- [1] K. Kaneko, in *Theory and Applications of Coupled Map Lattices*, edited by K. Kaneko (Wiley, Chichester, 1993).
  - [2] A. Pikovsky, M. Rosenblum, J. Kurths and S. Strogatz, *Synchronization: A universal concept in nonlinear sciences*, (CUP, Cambridge 2001); S. Boccaletti, J. Kurths, G. Osipov, D.L. Valladares and, C.S. Zhou, Phys. Rep. **366**, 1 (2002).
  - [3] N. Platt, E.A. Spiegel and C. Tresser, Phys. Rev. Lett. **70**, 279 (1993).
  - [4] J.F. Heagy, N. Platt and S.M. Hammel, Phys. Rev. E **49**, 1140 (1994); H.L. Yang and E.J. Ding, Phys. Rev. E **54**, 1361 (1996).
  - [5] A. Čenys, A. Namajūnas, A. Tamaševičius and T. Schneider, Phys. Lett. A **213**, 259 (1996); M. Sauer and F. Kaiser, Phys. Lett. A **243**, 38 (1998).
  - [6] S.C. Venkataramani, T.M. Antonsen Jr., E. Ott and J.C. Sommerer, Physica D **96**, 66 (1996).
  - [7] P.M. Gade and C.-K. Hu, Phys. Rev. E **60**, 4966 (1999); P.M. Gade, H.A. Cerdeira and R. Ramaswamy, Phys. Rev. E **52**, 2478 (1995).
  - [8] C. Anteneodo, S.E. de S. Pinto, A.M. Batista and R.L. Viana, Phys. Rev. E **68**, 045202(R) (2003); *ibid.* **69**, 029904(E) (2003).
  - [9] C. Anteneodo, A.M. Batista and R.L. Viana, Phys. Lett. A **326**, 227 (2004).
  - [10] P.G. Lind, J. Corte-Real, J.A.C. Gallas, Phys. Rev. E **69**, 026209 (2004).
  - [11] M. Ding and W. Yang, Phys. Rev. E **56**, 4009 (1997).
  - [12] C. Grebogi, S.M. Hammel, J.A. Yorke and T. Sauer, Phys. Rev. Lett. **65**, 1527 (1990); C. Zhou and J. Kurths, Phys. Rev. Lett. **88**, 230602 (2002).
  - [13] J.-P. Eckmann and D. Ruelle, Rev. Mod. Phys. **57**, 617 (1985).
  - [14] C. Anteneodo, Phys. Rev. E **69**, 016207 (2004).
  - [15] A. Prasad and R. Ramaswamy, Phys. Rev. E **60**, 2761 (1999).
  - [16] J. Theiler and L.A. Smith, Phys. Rev. E **51**, 3738 (1995).
  - [17] S. Dawson, C. Grebogi, T. Sauer, and J.A. Yorke, Phys. Rev. Lett. **73**, 1927 (1994); T.D. Sauer, Phys. Rev. E **65**, 036220 (2002).
  - [18] R.L. Viana, S.E. de S. Pinto, J.R.R. Barbosa and C. Grebogi, Int. J. Bifurcat. Chaos **13**, 3235 (2003).
  - [19] R. L. Viana, C. Grebogi, S. E. de Souza Pinto, S. R. Lopes, A. M. Batista, and J. Kurths, Phys. Rev. E **68** (2003).